1× N Multimode Interference Beam Splitter Design Techniques for On-Chip Optical Interconnections — Source link 🔗

Amir Hosseini, David Kwong, Yang Zhang, Harish Subbaraman ...+2 more authors

Institutions: University of Texas at Austin

Topics: Beam splitter, Splitter and Silicon photonics

Related papers:

- Optical multi-mode interference devices based on self-imaging: principles and applications

- On the design of 1xN multimode interference coupler for photonic integrated circuits

- A new design approach to large input/output number multimode interference couplers and its application to low-crosstalk WDM routers

- Simulation of an Ultra-Compact Multimode Interference Power Splitter Based on Kerr Nonlinear Effect

- Optical processor using waveguide holograms in multimode interference (MMI) couplers

1× N Multimode Interference Beam Splitter Design Techniques for On-Chip Optical Interconnections

Amir Hosseini, *Student Member, IEEE*, David N. Kwong, Yang Zhang, Harish Subbaraman, Xiaochuan Xu, and Ray T. Chen, *Fellow, IEEE*

Abstract—We derive an analytical relation for the maximum number of output channels for high-performance multimode interference (MMI)-based 1 × N optical beam splitters for a given MMI width. Using eigenvalue-expansion-based simulation results, we validate the analytical relation. Experimental data from MMIs fabricated on silicon nanomembrane also confirm the effectiveness of the design methodology for on-chip optical beam splitter designs.

Index Terms—Multimode interference coupler, optical interconnects, optical, silicon photonics, waveguide theory.

I. INTRODUCTION

ON-CHIP optical interconnections are being considered as a solution for the looming interconnection bottlenecks of limited bandwidth and large latencies. A network of on-chip optical interconnects in integrated photonic circuits (PICs) needs efficient optical beam-splitting and beam-shaping components as building blocks.

The self-imaging properties of multimode optical waveguides have been utilized in $N \times M$ multimode interference (MMI) couplers. The theory of self-imaging in multimode optical waveguides has been the subject of several studies [1]–[6]. The resolution and contrast of the images formed in the multimode waveguide determine the uniformity and insertion loss (or equivalently the total transmitted power) of MMI splitter devices [1]. It has been shown that $1 \times N$ MMI couplers with a large number of outputs (N) normally result in poor output uniformity and high insertion loss [2]. It has been shown that optimizing the core/cladding index contrast [2], [3] can improve the MMI performance.

A design methodology is required for on-chip high-performance MMIs for which the choice of tuning index contrast is not an option. Additionally, despite the advances in computer-aided design (CAD) tools for integrated electronic components, there has been little work on design tools for on-chip optical

components. We aim to find design rules that can be reliably used for on-chip efficient beam splitters without the need for time-consuming and computationally expensive simulations for each individual component.

In this paper, we first analyze the modal phase errors in symmetrically excited $1 \times N$ MMIs by investigating the modal dispersion relations. Then, we present a technique to minimize deviations of the modal dispersion relations from those required for ideal self-imaging. Finally, we derive a relation for the maximum number of output channels for a given MMI width that can still result in an acceptable MMI performance.

Silicon nanomembrane-based optical devices in silicon-on-insulator (SOI) substrates can be integrated with silicon electronics using techniques such as localized substrate removal [7]. Localized oxidized SOI from bulk silicon has been also used as potential platform to integrate silicon photonics and electronics [8]. We designed and fabricated several MMIs based on silicon nanomembrane rib waveguides. Experimental results show that the analytical formulas derived in this paper can be used as guidelines for on-chip MMI designs. Therefore, the presented design methodology can be easily implemented in CAD tools.

II. MAXIMUM NUMBER OF OUTPUT CHANNELS

Fig. 1 shows a schematic of a $1 \times N$ MMI splitter. The multimode waveguide section consists of a W_{MMI} wide and L_{MMI} long core with refractive index n_c. In the case of channel waveguides, an equivalent 2-D representation can be made by techniques such as the effective index method or the spectral index method [7]. W_w is the input/output channel waveguide width. Assume that n_{eff} is the effective index of the fundamental mode of an infinite slab waveguide with same thickness and claddings. For each mode p ($0 \leq p \leq M$) of an MMI that can support ($M + 1$) modes, the dispersion relation is given as [1]

$$\beta_m^2 + \kappa_{xp}^2 = \left(\frac{2\pi n_{\mathrm{neff},\mathrm{1\text{-}D}}}{\lambda_0}\right)^2 \tag{1}$$

where β_m is the propagation constant of the mth mode, λ_0 is the free-space wavelength. κ_{xm} is the lateral wave number of the mth mode given as $\kappa_{xm} = \pi(m + 1)/W_e$ where W_e is the effective width including the penetration depth due to the Goose–Hahnchen shift [4]. We use the effective width for generality; however, due to the high index contrast, $W_e = W_{\mathrm{MMI}}$ is a good approximation in silicon photonics. $n_{\mathrm{eff},\mathrm{1\text{-}D}}$ is the effective index of the fundamental mode of an infinite slab waveguide with same thickness and claddings from the effective index method. In the theory of self-imaging, β_m is approximated from (1)
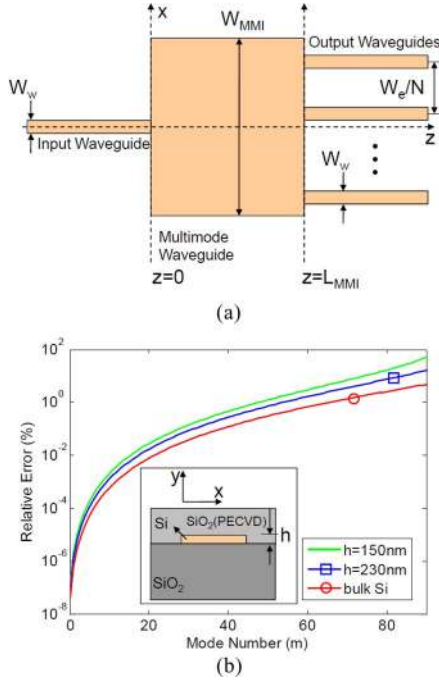
Fig. 1. (a) Schematic of a $1 \times N$ MMI beam splitter. Inset is a cross-sectional schematic of the SOI waveguiding structure. $n_{\mathrm{Si}} = 3.47$, $n_{\mathrm{SiO2}} = 1.45$, $n_{\mathrm{SiO2(PECVD)}} = 1.46$. (b) Relative error in calculation of modal propagation constant β_m when evaluated using (2) compared to the exact values from (1), for $W_{\mathrm{MMI}} = 30$ μm and $\lambda_0 = 1.55$ μm for different silicon nanomembrane thicknesses (h) and bulk silicon (infinite h). A schematic of the waveguide structure cross section is shown in the inset.

as [1]

$$\beta_m \approx \beta_0 - \frac{m(m-2)}{3L_\pi} \qquad (2)$$

where $L_\pi = \pi/(\beta_0 - \beta_1) \approx 4 n_{\mathrm{eff,1\text{-}D}} W_e{}^2 / 3\lambda_0$. Note that the β_m values given by (2) are necessary for ideal self-imaging at the output of the MMI coupler. In the case of symmetric excitation, such as a $1 \times N$ coupler excited by the fundamental mode of the input waveguide, using the approximation in (2), one can show that the required length for such a coupler is $L_{\mathrm{MMI}} = 3iL_\pi/4N$, where i is an integer.

This approximation results in errors in evaluated β_m values, as shown in Fig. 1(b). Interestingly, as the thickness of the silicon nanomembranes is reduced, the error introduced by the approximation becomes larger. Therefore, addressing the induced phase errors is more critical in rib silicon waveguides than in the case of ridge waveguides, such as the ones investigated in [9].

When using (2), the error in the calculated propagation constant can be estimated by the third term in the Taylor Expansion of β_m, given by (1) as $\Delta\beta_m \approx 2(\kappa_{xm}\lambda_0/4\pi n_{\mathrm{eff,1\text{-}D}})^4$. Deviation of the propagation constant values from those needed for ideal self-imaging results in deviation of the phase values φ_m of the modes propagating inside the multimode waveguide at the output of the MMI coupler from the modal phase values needed for ideal self-imaging. After propagating along the MMI, the

resulting modal phase errors at the output are given as

$$\Delta\phi_m = \Delta\beta_m L_{\mathrm{MMI}} = \frac{\pi\lambda_0^2(m+1)^4}{64N n_{\mathrm{eff,1\text{-}D}}^2 W_e^2}. \qquad (3)$$

For a high-quality image, we restrict the maximum $\Delta\varphi_m$ to $\pi/2$, which gives q, which is the maximum allowed mode number p. Note that for single-fold self-imaging, all φ_m values must be integer multiples of 2π. Thus, modal phase errors $\Delta\varphi_m > \pi/2$ flip the sign of the real part of the modal fields. In the case of multifold self-imaging, the restriction is not less severe. The numerical simulations of the MMI coupler performance confirm the effectiveness of the restriction of the maximum allowed modal phase error to $\pi/2$.

We choose W_w so that the highest order mode excited in the multimode region can satisfy this restriction. To do so, we pick W_w to be equal to the lateral wavelength $(2\pi/\kappa_{xq})$ of the highest allowed mode given by $\Delta\varphi_m < \pi/2$. In the case of modes for which $m \gg q$, the resulting modal phase errors are large. However, letting $W_w = 2\pi/\kappa_{xq}$ guarantees negligible excitation. Because several periods of these modes fall within the input excitation field, the resulting overlap integrals are thus negligible. For the other modes with order higher than q (for example, with orders $q + 2$, $q + 4$. etc.) that have a period that is just a little smaller than the input excitation field, the excitation is not negligible, but is little less than that of the mode q. However, the modal phase error values are just little larger than $\pi/2$ as well. By equating $W_{w,\mathrm{min}} = 2\pi/\kappa_{xq}$, we get

$$W_{w,\mathrm{min}} = \frac{1}{\sqrt[4]{2N}}\sqrt{\frac{\lambda_0 W_e}{n_{\mathrm{eff,1\text{-}D}}}}. \qquad (4)$$

$W_{w,\mathrm{min}}$ decreases as N increases. This is due to the fact that MMI's length decreases linearly with increasing N. Therefore, the accumulated phase errors $\Delta\varphi_m = L_{\mathrm{MMI}}\Delta\beta_m$ are also reduced with increasing N. Increasing access waveguide width for improving MMI performance was proposed in [9] without any notes on how wide the access waveguides should be. Equation (4) gives the minimum W_w for an acceptable MMI performance in terms of the insertion loss and output uniformity.

We note that that the output channel-to-channel spacing is W_e/N. Therefore, we can derive an upper bound on the maximum number of channels for which the image quality is still acceptable by $W_{w,\mathrm{min}} < W_e/N$ given as

$$N_{\mathrm{max}} \leq \left\lfloor \sqrt[3]{\frac{2 n_{\mathrm{eff,1\text{-}D}}^2 W_e^2}{\lambda_0^2}} \right\rfloor. \qquad (5)$$

The result is quite general (optimistic) and gives an upper bound for N_{max} for any waveguiding structure. For more realistic N_{max}, one needs to consider

$$N_{\mathrm{max}} \leq \left\lfloor \frac{W_e}{W_{w,\mathrm{min}} + s_{\mathrm{min}}} \right\rfloor \qquad (6)$$

where s_{min} depends on the waveguiding structure and is the minimum required side-to-side spacing between the output waveguides to avoid channel-to-channel coupling and/or required by the geometrical restrictions of the devices connected to the
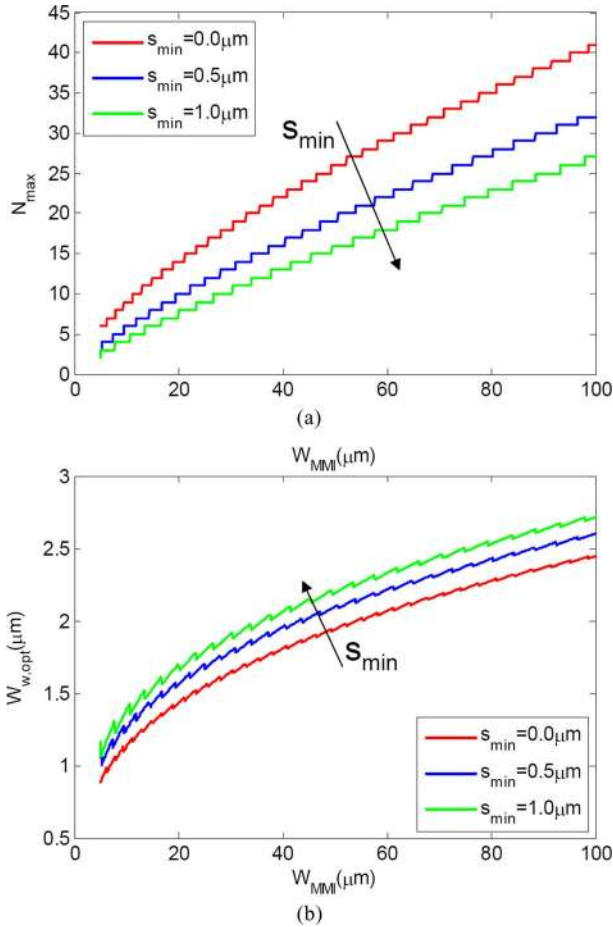
TABLE I
$1 \times N$ MMI-BASED OPTICAL BEAM SPLITTERS' LENGTH AND CHANNEL
WIDTH DIMENSIONS FOR $h = 230\,\text{nm}$ AT $\lambda_0 = 1.55\,\mu\text{m}$ (L_{MMI} VALUES
ARE CALCULATED USING $L_{\text{MMI}} = 3rL_\pi/4N$)

N	W_{MMI} (μm)	L_{MMI} (μm)	$W_{w,\text{min}}$ (μm)	W_w (μm)
6	30	276	2.16	2.16
8	30	207	2.02	2.02
10	30	166	1.91	1.91
12	30	138	1.83	1.50
14	30	118	1.76	1.14
16	30	104	1.70	0.88

Fig. 2. (a) Variation of the maximum number of the output channels versus MMI width. (b) Variations of the optimum channel width for $1 \times N_{\text{max}}$ MMIs versus MMI width.

MMI's output channels, as well as the limitations of the fabrication technique.

Fig. 2(a) shows N_{max} as a function of W_{MMI} for $s_{\text{min}} = 0$ (5), $s_{\text{min}} = 0.5\,\mu\text{m}$, and $s_{\text{min}} = 1.0\,\mu\text{m}$. $n_{\text{eff},1\text{-D}} = 2.85$, which corresponds to $h = 230\,\text{nm}$ at $\lambda_0 = 1.55\,\mu\text{m}$ in Fig. 1(b) inset. $s_{\text{min}} = 1.0\,\mu\text{m}$ is chosen to avoid optical coupling in thin silicon rib waveguides of the MMIs' outputs and also to minimize the effects of the proximity effect during the e-beam writing as presented. Fig. 2(b) demonstrates variations of $W_{w,\text{min}}$ versus W_{MMI} for an MMI with N_{max} output channels.

From (5), N_{max} is a sublinear function of W_{MMI} even in the most optimistic case, where $s_{\text{min}} = 0$. This is also evident from Fig. 2. In other words, if an MMI design with W_{MMI} and N results in a good MMI performance, in general, an MMI design with RW_{MMI} and RN does not necessary exhibit a good performance, where R is an integer number equal to or greater than 2. This is an important consideration for scalability of MMI-based devices.

Equations (4) and (5) guarantee good MMI performance without a need to apply the other performance-enhancing techniques such as index contrast tuning [2], [10], multimode section input taper [3], or L_{MMI} and output access waveguide position optimization [11]. We will investigate this claim using eigen-

mode decomposition-based simulations in Section III and rib waveguide MMIs in Section IV.

III. SIMULATIONS AND DISCUSSIONS

In order to investigate the effect of W_w on the quality of the N-fold self-imaging, we used the eigenmode expansion (EME) simulator in the FIMMPROP module from Photon Design. The EME method is based on a rigorous solution of Maxwell's equations, and therefore, the results approach the exact solution for a large number of modes in the expansion. The algorithm is inherently bidirectional and fully vectorial [13]. We assumed SOI substrate as shown in Fig. 1 inset, where the thickness of the silicon slab is $h = 230\,\text{nm}$, $n_{\text{Si}} = 3.47$, $n_{\text{SiO2}} = 1.45$, $n_{\text{SiO2(PECVD)}} = 1.46$, and $n_{\text{eff},1\text{-D}} = 2.85$. Throughout this paper, $\lambda_0 = 1.55\,\mu\text{m}$.

Let us consider MMIs with $W_{\text{MMI}} = 30\,\mu\text{m}$ and with required $s_{\text{min}} = 1.0\,\mu\text{m}$ and different N (see Table I). The maximum number of outputs for which [see Fig. 2(a)] high-quality self-imaging of the input is possible is $N_{\text{max}} = 11$. For any $N > 11$, the condition $W_{w,\text{min}} < W_e/N - s_{\text{min}}$ cannot be fulfilled. In other words, W_w is forced to be smaller than the $W_{w,\text{min}}$ value from (4), as indicated in Table I.

Fig. 3(a)–(f) shows the output field [abs(E_x)] profile of 1×6, 1×8, 1×10, 1×12, 1×14, and 1×16 MMIs, respectively. Fig. 3(g) and (h) shows the insertion loss and the output uniformity, respectively. Insertion loss is the ratio of the total output power to the input power. Uniformity is calculated as $10\log(P_{\text{min}}/P_{\text{max}})$, where P_{max} and P_{min} are the maximum and minimum power (norm of the fundamental mode) of the MMI output channels, respectively. In our simulations, we let 75 modes to propagate in the multimode section. We noticed that increasing the number of modes resulted in less than 0.1% difference in the calculated insertion loss and uniformity values.

Fig. 3 shows that as N increases, the degradation in the MMI performance is minimal as long as $W_w = W_{w,\text{min}}$. However, as W_w becomes increasingly smaller than the required $W_{w,\text{min}}$, the MMI performance is rapidly degraded due to increasing phase errors discussed before. One can note that the predicted $N_{\text{max}} = 11$ from (6) corresponds to the "knee point" in both the output uniformity and insertion loss versus the number of output channels (N). Therefore, the EME simulations are in good agreement with the theoretical predictions.
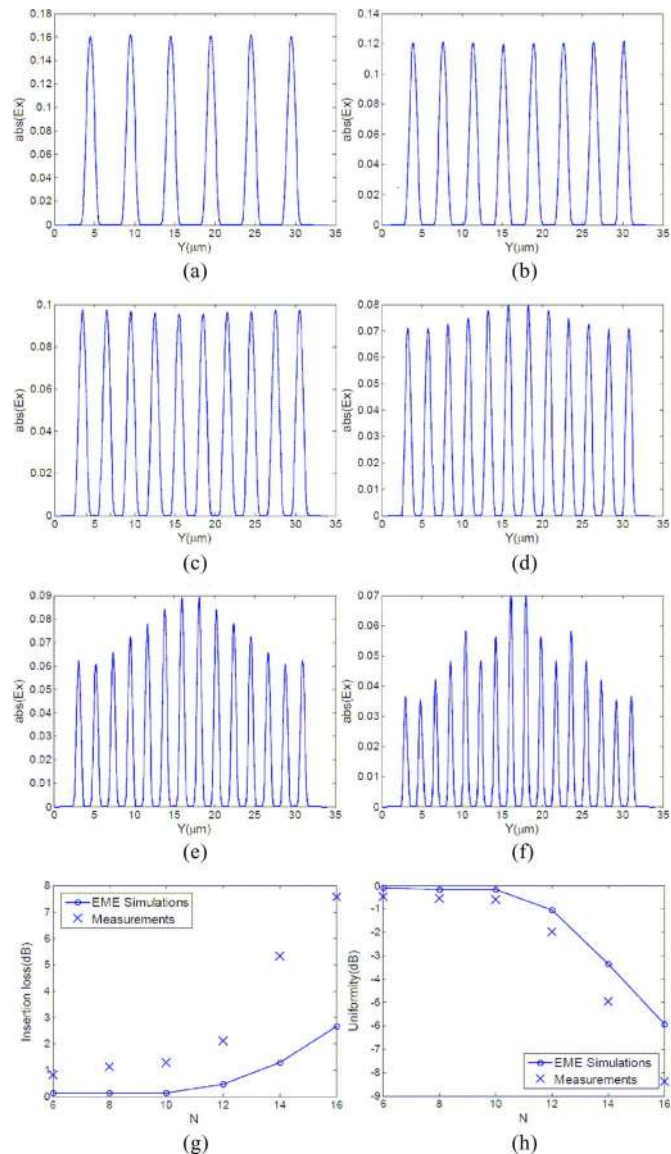
Fig. 3. (a)–(d) abs(E_x) at the MMIs' outputs in the middle of the output channel (height-wise). (e) Total (all channels) output power (normalized with respect to the input power) versus the output channel number (N). (f) Output uniformity versus output channel number.
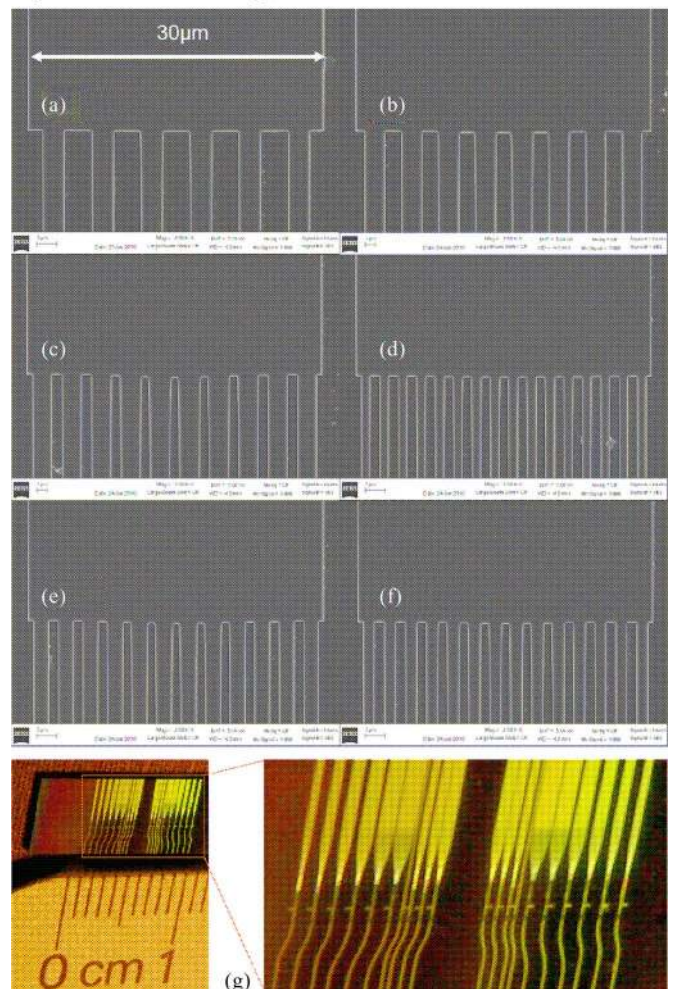

Fig. 4. SEM pictures of the fabricated SOI-based MMIs: (a) 1×6, (b) 1×8, (c) 1×10, (d) 1×12, (e) 1×14, and (f) 1×16. (g) Picture of the entire chip showing different MMI devices. The input s-bends and the fanned-out output channels are on the bottom and top sides of the chip, respectively.

IV. EXPERIMENTAL DATA FROM RIB WAVEGUIDES

We fabricated 1×6, 1×8, 1×10, 1×12, 1×14, and 1×16 MMIs ($W_{\mathrm{MMI}} = 30~\mu\mathrm{m}$) with W_w and L_{MMI} values shown in Table I. The MMIs are fabricated on a SOI substrate with 3-μm buried oxide layer and 250-nm top silicon layer. Light oxidation creates a 45-nm top oxide layer that will serve as an etch mask. This oxidation consumes 20 nm of silicon, giving a final silicon layer of 230 nm. The MMIs are patterned using a JEOL JBX600 electron beam lithography system, followed by an HBr/Cl$_2$-based reactive ion etching and plasma-enhanced chemical vapor deposition (PECVD) of a 1-μm thick silicon dioxide film for the top cladding. The refractive index of this PECVD cladding film was found to be $n_{\mathrm{PECVD}} = 1.46$.

All the input and output channels are tapered to 2.50 μm to match the output coupling lensed fiber. There is an s-bend before each MMI input to avoid background noise from the input fiber during characterization of the output channels' near field. The output channels are fanned out for 30-μm center-to-center separation so that we are able to capture clear images of the near field at the output waveguide facets using a $10\times$ IR lens. SEM pictures of the fabricated MMIs and a picture of the SOI chip are shown in Fig. 4.

Transverse electric field from an external cavity tunable laser source is coupled into the input waveguides through a tapered and lensed polarization maintaining fiber. A CCD camera, connected to a tunable magnification IR lens (max $10\times$), captured top-down images of the scattered light at the cleaved output waveguide facets as shown in Fig. 5.

In order to characterize the MMIs' performance, a single-mode output fiber is scanned at output side across each output channel cross section for maximum output coupling. At least two samples of each MMI are tested. The results of the fiber-scanning measurements are summarized in Fig. 3(g) and (h). As shown in Fig. 3(g) and (h) and 5(a)–(f), the MMIs' performance
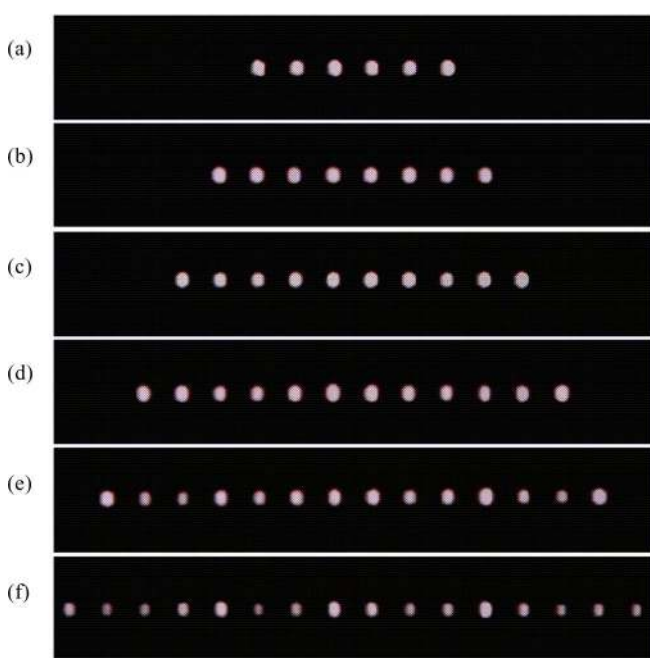
[7] S. Sridaran and S. A. Bhave, "Nanophotonic devices on thin buried oxide silicon-on-insulator substrates," *Opt. Express*, vol. 18, pp. 3850–3857, 2010.

[8] N. Sherwood-Droz, A. Gondarenko, and M. Lipson, "Oxidized silicon-on-insulator (OxSOI) from bulk silicon: A new photonic platform," *Opt. Express*, vol. 18, pp. 5785–5790, 2010.

[9] Y. Shi, D. Dai, and S. He, "Improved performance of a silicon-on-insulator-based multimode interference coupler by using taper structures," *Opt. Commun.*, vol. 253, pp. 276–282, 2005.

[10] R. Yin, J. Yang, X. Jiang, J. Li, and M. Wang, "Improved approach to low-loss and high-uniformity MMI devices," *Opt. Commun.*, vol. 181, pp. 317–321, 2000.

[11] Q. Wang, J. Lu, and S. He, "Optimal design of a multimode interference coupler using a genetic algorithm," *Opt. Commun.*, vol. 209, pp. 131–136, 2002.

[12] D. F.G. Gallagher and T. P. Felici, "Eigenmode expansion methods for simulation of optical propagation in photonics—Pros and cons," *Proc. SPIE*, vol. 4987, pp. 69–82, 2003.

Fig. 5. Top-down IR images of MMI output waveguides' facets for (a) 1 × 6, (b) 1 × 8, (c) 1 × 10, (d) 1 × 12, (e) 1 × 14, and (f) 1 × 16. The channel-to-channel separations at the output facet is 30 μm in all cases.

rapidly degrades with the number of output channels for $N > 11$. Therefore, experiments also validate the theoretical predictions.

V. Conclusion

We derived a design rule for the maximum number of output channels of MMI-based beam splitters for a given MMI width. Highly accurate EME simulations confirmed the analytical relations for the maximum output channel number. Optical characterization of MMI beam splitter devices fabricated on SOI using silicon nanomembranes experimentally demonstrates the validity of the theoretical predictions for the maximum output channel number. Equations (4)–(6) can be used as a guideline for high-performance on-chip optical beam splitter design.

References

[1] R. Ulrich and T. Kamiya, "Resolution of self-images in planar optical waveguides," *J. Opt. Soc. Amer.*, vol. 68, pp. 583–592, 1978.

[2] J. Z. Huang, R. Scarmozzino, and R. M. Osgood Jr., "A new design approach to large input/output number multimode interference couplers and its application to low-crosstalk WDM routers," *IEEE Photon. Technol. Lett.*, vol. 10, no. 9, pp. 1292–1294, Sep. 1998.

[3] R. M. Lorenzo, C. Llorenle, E. J. Abril, and M. López, "Improved self-imaging characteristics in 1 × N multimode couplers," *Proc. Inst. Elect. Eng. Optoelectron.*, vol. 145, no. 1, pp. 65–69, 1998.

[4] L. Soldano and E. Pennings, "Optical multimode interference devices based on self-imaging: Principles and applications," *J. Lightw. Technol.*, vol. 13, no. 4, pp. 615–627, 1995.

[5] M. Rajarajan, B. Rahman, T. Wongcharoen, and K. Grattan, "Accurate analysis of MMI devices with two-dimensional confinement," *J. Lightw. Technol.*, vol. 14, no. 9, pp. 2078–2084, 1996.

[6] A. Hosseini, D. N. Kwong, C.-Y. Lin, B. S. Lee, and R. T. Chen, "Output formulation for symmetrically-excited one-to-n multimode interference coupl," *IEEE J. Selected Topics Quantum Electron.*, vol. 6, no. 1, pp. 53–60, Feb. 2010.

Amir Hosseini (S'05) received the B.Sc. degree in electrical engineering from the Sharif University of Technology, Tehran, Iran, in 2005, and the M.S. degree in electrical and computer engineering from Rice University, Houston, TX, in 2007. He is currently working toward the Ph.D. degree in Dr. Ray T. Chen's Optical Interconnect Group at the Department of Electrical and Computer Engineering, University of Texas, Austin.

He is engaged in research on modeling, design, fabrication, and characterization of optical phased array technology and high-performance optical modulators. His main focus is on the design optimization for micro- and nanoscale manufacturability. He has authored/coauthored more than 50 peer-reviewed technical papers. His research interests include physical layer modeling and characterization for network on chip, alternative solutions for high-performance on-chip interconnects.

Mr. Hosseini is a 2010 Microsoft Fellowship finalist, a Prince of Wales' scholar, and a member of Phi Kappa Phi and Tau Beta Pi.

David N. Kwong received the B.S. and M.S. degrees in electrical engineering from the University of Texas (UT), Austin, in 2006 and 2010, respectively. He is currently working toward the Ph.D. degree in Dr. Ray T. Chen's Optical Interconnect Group at the Department of Electrical and Computer Engineering, UT.

In 2006, he was with Samsung Austin Semiconductor in process integration for DRAM back end of line (BEOL) processes. His research interests include silicon nanophotonic devices for optical interconnects and optical phased arrays.

Yang Zhang received the B.S. degree in optoelectronics in 2007 and the M.S. degree in optical engineering in 2009, both from the Huazhong University of Science and Technology, Wuhan, China. He is currently working toward the Ph.D. degree in Dr. Ray T. Chen's Optical Interconnect Group at the Department of Electrical and Computer Engineering, University of Texas, Austin.

His research interests include nanoscale waveguides and devices for optical interconnect.

Harish Subbaraman received the M.S. and Ph.D. degrees in electrical engineering from the University of Texas, Austin, in 2006 and 2009, respectively.

With a strong background in RF photonics and X-band phased array antennas, he has been working on true-time-delay feed networks for phased array antennas and carbon nanotube-based thin-film transistors for the last 4 years. He has served as a PI for three SBIR/STTR Phase I/II projects from NASA, Air Force, and Navy. He has more than 15 publications in refereed journals and conferences.

Xiaochuan Xu received the B.Sc. and M.S. degrees in electrical engineering from the Harbin Institute of Technology, Harbin, China, in 2006 and 2009, respectively. He is currently working toward the Ph.D. degree in Dr. Ray T. Chen's Group at University of Texas, Austin.

Ray T. Chen (F'04) received the B.S. degree in physics from National Tsing-Hua University, Taiwan, in 1980, the M.S. degree in physics from the University of California, San Diego, in 1983, and the Ph.D. degree in electrical engineering from the University of California, Irvine, in 1988.

He worked as a Research Scientist, a Manager, and the Director of the Department of Electrooptic Engineering in Physical Optics Corporation, Torrance, CA, from 1988 to 1992. He joined the University of Texas (UT), Austin, as a Faculty Member to start optical interconnect research program in the Department of Electrical and Computer Engineering in 1992. He holds the Cullen Trust for Higher Education Endowed Professorship at UT and the Director of Nanophotonics and Optical Interconnects Research Laboratory, Microelectronics Research Center. He is also the Director of a newly formed AFOSR Multidisciplinary Research Initiative (MURI) Center for Silicon Nanomembrane involving faculty from Stanford, UIUC, Rutgers, and UT. He also served as the CTO/founder and the Chairman of the Board of Radiant Research from 2000 to 2001 where he raised 18 million dollars A-Round funding to commercialize polymer-based photonic devices involving more than 20 patents, which was acquired by Finisar in silicon valley (NASDAQ: FNSR). He also serves as the founder and the Chairman of the Board of Omega Optics, Inc., since its initiation in 2001. More than 5 million dollars of research funds were raised for Omega Optics. His research work has been awarded with 101 research grants and contracts from sponsors such as DOD, NSF, DOE, NASA, EPA, NIH, the State of Texas, and private industry. There are 35 students who have received the EE Ph.D. degree from his research group at UT Austin. His group has reported its research findings in more than 560 published papers including more than 70 invited papers. He holds 20 issued patents. His research topics are focused on nanophotonic passive and active devices for optical phased array and interconnect applications, thin film guided-wave optical interconnection and packaging for 2-D and 3-D laser beam routing and steering, and true time delay wide band phased array antenna.

Dr. Chen has chaired or been a program committee member for more than 100 domestic and international conferences organized by the IEEE, the SPIE, the OSA, and the PSC. He has served as an editor or coeditor for 18 conference proceedings. He has also served as a consultant for various federal agencies and private companies and delivered numerous invited talks to professional societies. He is a Fellow of the OSA and the SPIE. He was the recipient of the 1987 UC Regent's Dissertation Fellowship and of the 1999 UT Engineering Foundation Faculty Award for his contributions in research, teaching, and services. He is also the recipient of the 2008 IEEE Teaching Award and of the 2010 Best Research Professor Award from the IEEE and HKN Honor Society. In his undergraduate years in National Tsing-Hua University, he led a university debate team in 1979 which received the National Championship of National Debate Contest in Taiwan.